Fusion Engineering and Design 223 (2026) 115553

Contents lists available at ScienceDirect

Fusion Engineering and Design

journal homepage: www.elsevier.com/locate/fusengdes

Preliminary assessment of surface inspection using visual imaging sensors for DEMO service weld seam☆

A. Azka

Karlsruhe Institute of Technology, Kaiserstraße 12, Karlsruhe, 76131, Germany

ARTICLE INFO

Keywords:
DEMO
Non-destructive examination
Remote maintenance
Visual inspection
Service joining

ABSTRACT

Maintenance of DEMO breeding blanket includes the removal and replacement of plasma facing components. Due to the components having an active cooling loop, multiple coolant pipes need to be removed to allow access to the tokamak. The connection then needs to be reconnected using the replacement components. To fulfill the safety requirements, the welded connection needs to be inspected and approved for operation. Due to the space restriction of DEMO vacuum vessel, both the welding procedure and the subsequent inspection procedure must be conducted from inside the pipe bore.

One of the methods currently under development in DEMO remote maintenance work package is visual inspection method designed to inspect the surface of the pipe weld seam as an alternative inspection method.

This study presents the comparison between stereo RGB cameras and laser triangulation-based system for use in demo service joining. This includes the comparison between the visual inspection systems for their capability to detect the pipe weld seam, detect any pipe weld defect if present and quantify the size of the pipe defect. With the result from each visual inspection system, a comparative advantage and disadvantage analysis of each sensor is carried out and the result of the analysis is then used for further development and integration of the inspection system into the overall cut and weld concept.

1. Introduction

During the maintenance phase of the DEMO power plant, multiple components which are entering their end of service time will be replaced with a new one. This includes the replacement of blankets and divertors which are plasma facing components [1], as shown in Fig. 1. Both divertor and breeding blankets are actively cooled components which are connected to the cooling loop through cooling pipes. Breeding blankets have additional pipes which are called purge pipes. Purge pipes are used to remove tritium from the breeding modules which are then processed further in an ex-vessel processing facility and will further be pumped back in as part of the D-T fuel cycle [2]. Both cooling and purge pipes needs to be disconnected to the plant loop before the removal of the divertors and breeding blankets (example of weld seam positions that needs to be serviced to access outboard BB is shown in Fig. 2), and both set of pipes needs to be reconnected with the plant loop before the power plant is allowed to operate. The strand which is responsible for this concept is called service joining and one of the concepts developed by the service joining strand of DEMO is the application of the cut and weld (C&W) concept for both cooling and purge pipes [3]. After a C&W procedure is carried out on the pipe an examination system of the weld beads needs to be developed to be able to commission the welded connection for operation, to ensure the safety aspect of these pipe connections.

During safety inspection of pipe connections, one of the aspects that is inspected is the surface condition of the pipes. To pass the safety requirements of the regulators, there are certain requirements that the pipes need to met to qualify. These requirements includes the condition of the weld, whether there are defects of certain types and sizes present on the surface. The requirements are regulated by industry standards such as RCC/RSE [4], ASME [5] or KTA [6] standards.

According to ASME-IX, the three types of examinations used during in-service inspection are defined as visual, surface, and volumetric [5]. Visual inspection covers inspection method using image and video capture sensor. A surface examination indicates the presence of surface discontinuities, which may be conducted using magnetic particle, liquid penetrant, eddy current, or ultrasonic method [7]. A volumetric examination indicates the presence of discontinuities throughout the volume of material and may be conducted from either the inside or outside surface of a component using methods such as radiographic, ultrasonic, eddy current, acoustic emission, or alternative examination methods [7]. Previous study on the allowable defect size which takes

☆ This article is part of a Special issue entitled: 'SOFT 2024' published in Fusion Engineering and Design.

E-mail address: azman.azka@kit.edu.

https://doi.org/10.1016/j.fusengdes.2025.115553
Received 29 December 2024; Received in revised form 5 November 2025; Accepted 30 November 2025
Available online 1 December 2025
0920-3796/© 2025 The Author. Published by Elsevier B.V. This is an open access article under the CC BY license (http://creativecommons.org/licenses/by/4.0/).

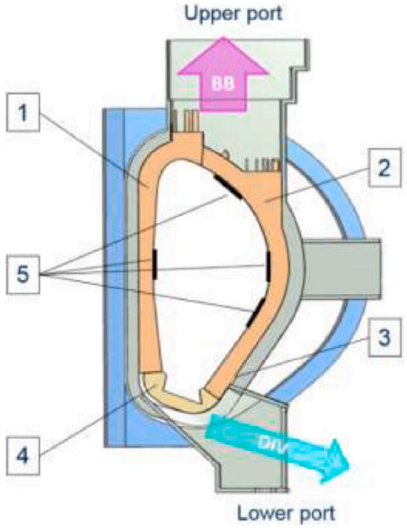

Fig. 1. Actively cooled in-vessel components such as breeding blankets (1 and 2) and divertor (4), which needs to be replaced during the maintenance phase [1].

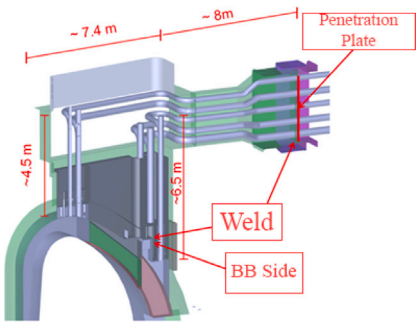

Fig. 2. Example of weld seams that needs to be serviced to access outboard breeding blanket for maintenance purposes.

into account the industry standard and numerical analysis has been carried out. From that study, the sensor requirement is to detect defects with a volumetric dimension of 1 mm^3 or larger with defect length of 0.5 mm or longer [8].

This study focuses on the investigation for possibility of using visual inspection sensors such as camera or laser to carry surface inspection. Such surface inspection is carried out by constructing of a surface map of the pipe interior using image depth map [9]. The surface map can then be used to evaluate the surface of the pipe. Using the surface map, overall pipe condition can be assessed manually or assisted using machine vision to detect surface defects or notable features that can pose safety threat to the overall power plant operation. The main goal is to compare the feasibility and characteristics of select visual sensors to generate a surface map.

2. Design consideration and test rig set-up

The visual sensors are compared against each other on a test rig constructed at KIT. The piping concept for DEMO upper port purge and cooling pipes restricts the deployment of sensors. All of the sensors that will be used for pipe inspection needs to be remote handling compatible and must be deployed with in-bore configuration.

The main objective of the test is the creation of a surface map.

Fig. 3. Weld sample produced from previous welding PoP test [10].

2.1. Pipe sample

Pipe samples provided by a Proof-of-Principle (POP) test conducted for welding head of DEMO pipes [10]. The welding head is tested on DN90 schedule 40 pipes which are representative of DEMO purge pipe diameter. The welded sample consists of two symmetrical flanged machined pipe sections welded together to form a pipe sample with length of 100 mm, as shown in Fig. 3.

2.2. Sensor selection

Sensors which are tested are visual sensors which are selected based on their suitability for in-bore use. The family of sensor that will be tested is visual imaging sensors such as camera and laser triangulation. The main criteria why visual imaging sensors are selected for this study is that the visual imaging sensors can be used as pathfinding and control sensor as well. Cameras and Laser does not need to have specific measuring configuration (unlike ultrasonic sensor which needs to have the sensor in contact with the wall, requiring the deployment system to have 2 configuration: deployment configuration and measuring configuration), can still measure while in motion (unlike dye penetrant which requires the deployment unit to be stationary), and doesnt require a receiver to be placed on the pipe out-bore. The possibility to use pathfinding sensors as inspection sensors would also present the possibility of having a more compact inspection system with simpler inspection procedure.

As the study is aimed to research on the capabilities of the sensors which are already available on the market, creating a custom sensor to fit the need of DEMO maintenance is beyond the scope of this preliminary study. Therefore, the sensors are selected that can fit inside a DN 90 pipe, the same pipe size that is used for weld head test trial [10].

The main categories of selection are availability, dimensions, and deployment considerations. Radiation resistance will considered for future testing to test sensor performance under radioactive condition. This include possibility of further sensor development and senor modification to meet radiation resistance requirement for deployment inside DEMO Bioshield. Sensors can be divided into two major categories, active sensors and passive sensors(as shown in Fig. 4).

2.2.1. Active sensor

Active sensors encompass sensors which use a signal sent by an emitter, which is then deflected by the test object and then captured by a receiver. This sensor family has the advantage of having high resistance to ambient noise and low ambient condition sensitivity, as the signal emitted can be attuned to cancel out the ambient noise. Major drawback of the concept is that the sensor requires at least one emitter and one receiver, making the overall sensor dimension larger than the passive sensors.

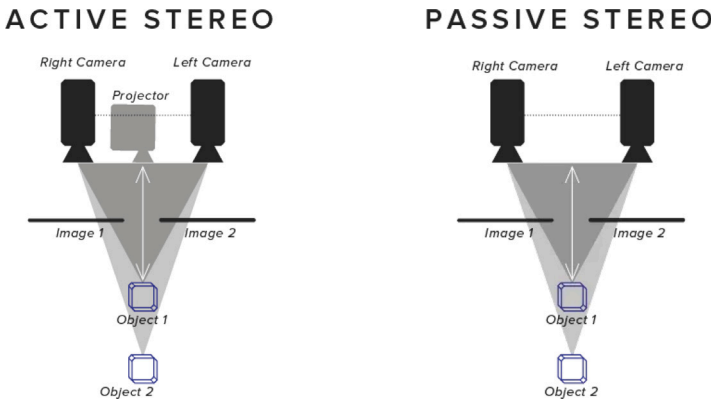

Fig. 4. Comparison between active (left) and passive (right) sensors, in this case of a stereo imager.

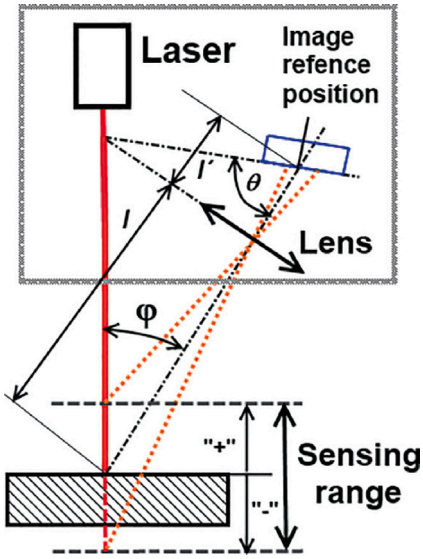

Fig. 5. Laser triangulation working mechanism.

Fig. 6. Citris annular laser line.

2.2.2. Passive sensor

Active sensors encompass sensors which use signals from the ambient environment captured by a receiver. This sensor family has the advantage of having simple construction and not having to rely on a signal emitted by an emitter. A major drawback of the concept is that the sensor is more sensitive to ambient condition and noise than active sensors.

2.3. Selected sensors

From families of sensors described on Section 2.2, three sensors were chosen: Intel D405, stereo IMX219-77, and circular laser CiTris 60-140.

Both the Intel D405 and stereo IMX219-77 sensors were used due to their compact size as well as their capability to output a depth data as well as RGB image using stereoscopy technology [11,12]. As neither system uses an additional emitter, both can be classified as passive systems. No active stereography systems is tested, since at the time of writing no readily available active system with two sensors and one projector/emitter is available on the market that can fit inside a DN90 pipe.

CiTris 60-140 is a circular laser measurement sensor using triangulation concept (as shown in Fig. 5) by emitting an annular laser light on the surface which is then read by a camera [13]. A circular sensor is chosen instead of a linear sensor due to deployment issue for linear sensor, as the deployment system needs to anchor on the pipe wall and move the linear sensor tangentially to be able to read the radial surface of the pipe. A circular laser sensor produce an annular surface reading using laser line as shown in Fig. 6 that can be stitched together with the corresponding odometry reading while only requiring the sensor to move axially along the pipe.

2.4. Test rig design

Pipe samples are placed on a PoP (Proof-of-Principle) test rig (as shown in Fig. 7) which consists of a straight stretch of pipe with an opening slot to drop the pipe sample in place (as shown in Fig. 8 (left)). The sensors are mounted on a deployment jig (as shown in Fig. 8 (right)), which then pulled using a set of pulleys and actuator along the pipe. The deployment jig is pulled at the constant speed of 12 mm/s by the linear actuator.

3. Result and discussion

From the measurement process some observations of the sensor performance have been made, which will be discussed in this chapter. It needs to be noted that during the measurement run of the sensors, no odometry data (from either rotary encoder or inertial measurement unit (IMU)) was taken with the measurement run. The effect of not including the odometry data is discussed in each subsection.

As mentioned in 2, the main objective of the test is the creation of a surface map. The surface map can then be compared and future improvements can be discussed.

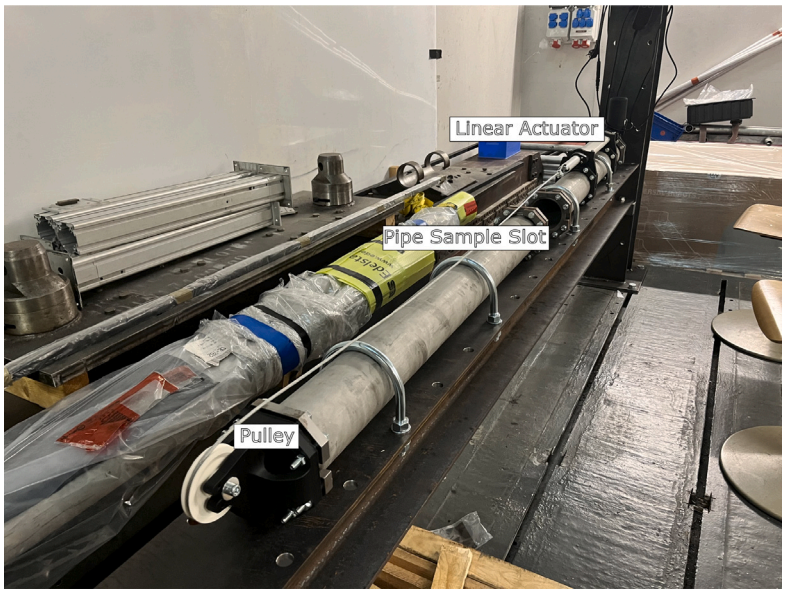

Fig. 7. Test rig used for testing the sensors.

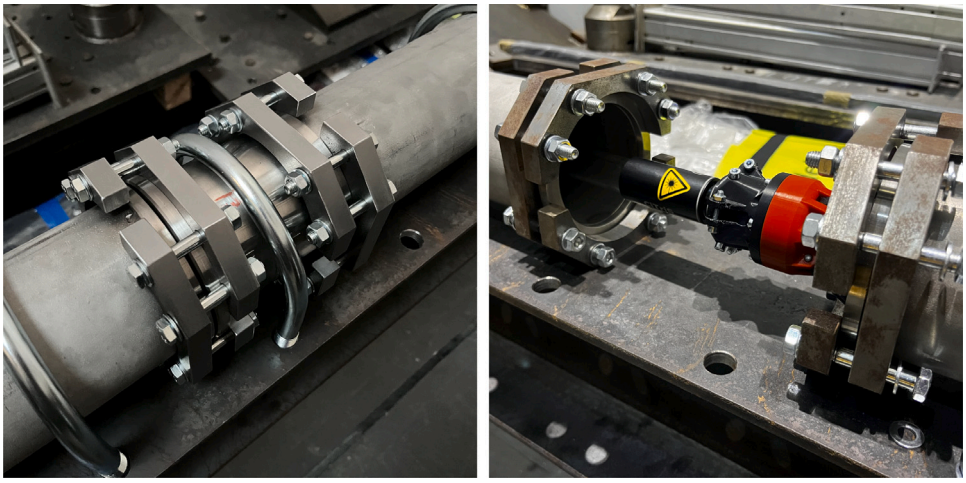

Fig. 8. Weld sample (left) and example of sensor deployed inside pipe (right).

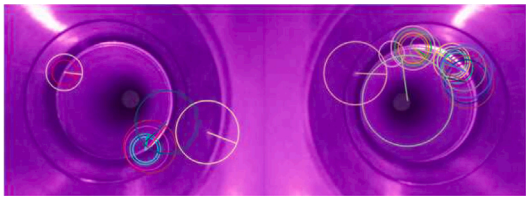

Fig. 9. Detected feature using OpenCV.

3.1. Stereovision cameras

From the test run using both Intel D405 and IMX219-77 sensors, with D405 using a RGB camera and a IR-Depth camera while IMX219-77 is using two TGB camera. Feature detection is used by the post-processing algorithm to merge and calculate disparity between left and right images [12,14]. The disparity is then converted into a depth profile of the features.

While IMX219-77 managed to capture images from the test pipe, images taken with the sensor proved to be difficult to process for triangulation and depth analysis. The measurement found using IMX219 in combination with OpenCV [15] shows a difficulty in finding any particular feature on the pipe surface that can be traced on both cameras. As shown in Fig. 9, the post-processing algorithm only manage to pick up features of the weld seam or where the sample pipe was mounted on the test rig. In addition to that, the features detected on one image does not match the feature well on the other image. This proved to be insufficient to provide a depth map of the pipe internal surface.

Therefore, to use the stereovision camera as means to construct surface map, further development of the feature detection, specifically for pipes, is required, as most of the readily available are not capable to detect the features on the pipe for feature matching algorithm to be used.

3.1.1. D405 with one RGB camera and one IR-Depth camera

The test run using D405 managed to produce a sample depth map. This is due to the in house image signal processor that Intel D405 uses [16]. As shown in Fig. 10, the sensor managed to pick up features

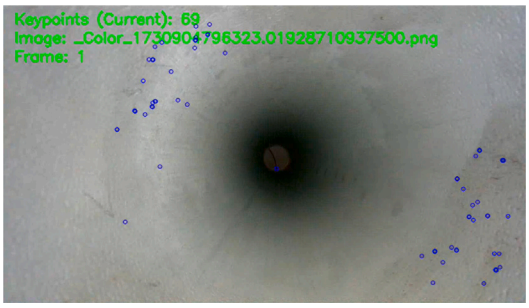

Fig. 10. Data points (blue) picked up by Intel D405 camera.

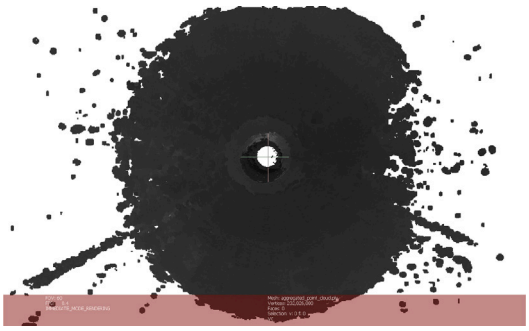

Fig. 11. Reconstructed data point using output from Intel D405 camera.

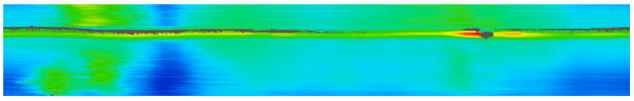

Fig. 12. Laser reading of the pipe sample.

on the plain pipe wall. While the data points per each image are sparse, the resulting data points from multiple images during a measurement run can be then stitched up to form a surface map, as shown on 11. Each pixels represent detected data points with inherent data such as local coordinate (in cartesian coordinate of x,y,z) and color information (in R,G,B triplets).

The sensor of D405 itself runs at frame rate of up to 90 frame/second [16]. Therefore with the assumption that the deployment has no slip and runs at a constant speed of 12 mm/second, the distance between frames is assumed to be 0.133 mm. From the test result, a uniform and equidistant annular data is assumed. However, from the measurement video taken at the same time as the image acquisition, there is some notable slip between the deployment unit and the pipe surface. This means that the accuracy of the measurement results needs to be validated in further study.

3.2. Laser triangulation sensor

Measurement runs using the laser triangulation sensor manages to produce a surface map of the pipe interior. The resulting surface map is shown in Fig. 12. A gray band is shown on the surface of the pipe where the weld seam is supposed to be located. This is due to the laser ring being obstructed by an obstacle and therefore the laser line cannot be transmitted to the receiver (the principle of is shown in Fig. 13).

An example of the measurement line is shown in Fig. 14, where data points between ±260° and ±270° lay outside the measurement range. The construction of CiTris means that the distance of the laser transmitter is fixed against the receiver. Therefore it is physically not possible to measure the obstructed area without changing the sensor head or redeploying the sensor in a different configuration.

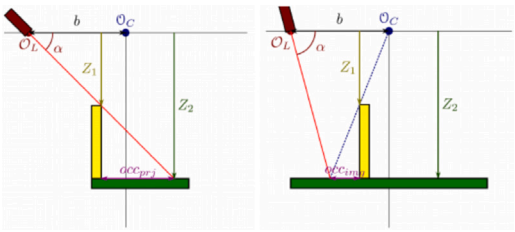

Fig. 13. Occlusion in a laser triangulation system where either the laser emitted from the emitter is blocked from the surface (left) or the laser reflected from surface is blocked from receiver (right) [17].

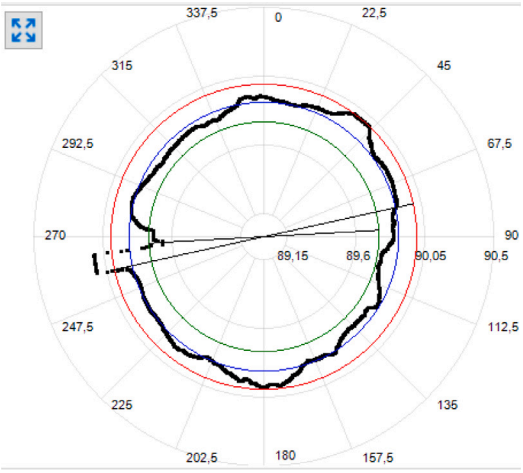

Fig. 14. Measurement of pipe surface with occlusion between ±260° and ±270°.

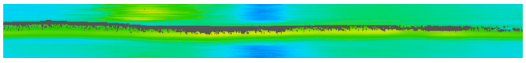

Fig. 15. Occlusion of weld toe.

This manifested in two particular occurrences of the occlusion. The first one is the occlusion of the weld toe (as shown on Fig. 15) due to the laser line obstructed by the weld face. The second one is the occlusion of the weld crater (as shown on Fig. 16). The occlusion of the weld crater prevents the measurement of the crater depth, therefore making the assessment of the criticality of the weld defect more difficult.

3.3. Surface map comparison

From the stitching process of the measurement result using both RGB-Depth camera (shown in Fig. 17) and laser triangulation (shown in Fig. 19), the odometry has to be given in order to carry the stitching process. For both processes, a surface map can be generated, which can be used to inspect the weld surface.

For the test result, a uniform and equidistant data is assumed to generate surface map using stitching. However, during of the measurement, a video recording was also taken. Qualitatively from observing the video, there are noticeable slips between the deployment unit and the pipe surface. This means that the accuracy of the measurement result is compromised. This necessitates the use of odometry to correct the position of the data point in case that slip happens. Therefore a further improvement of the workflow by integrating odometry based correction would be required.

The resulting data point cloud shows that the reconstruction is possible using the data points from the camera sensor and built image

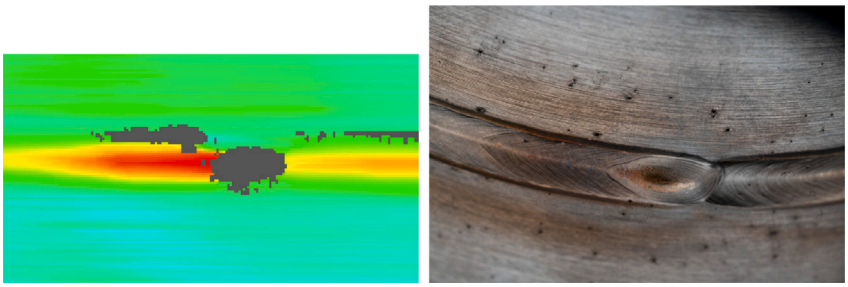

Fig. 16. Occlusion of weld crater (left) compared to the picture of the crater (right).

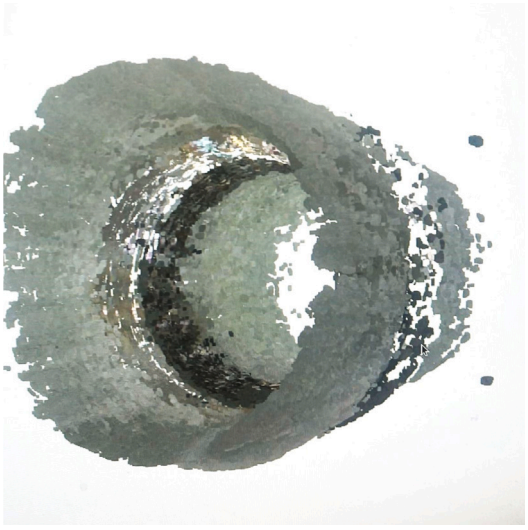

Fig. 17. Point cloud at weld sample after data point processing using Intel D405 camera.

signal processor with postprocessing using a Canny-like method [18]. However, the point cloud does not produce a surface map of the pipe internal surface, but rather a cloud around the surface. This is due to the condition of the pipe reflectivity, producing noise. Impact of surface finish of the pipe also shows on the result of the camera based measurement, as shown in Fig. 17 that the point cloud is more sparse at the area around pipe sample. This is due to, as noted in 2.1 that the pipe sample is made from machined stainless steel while the pipe section of the test bench, as noted in 2.4, is made from section of cold rolled pipe. Cold rolling produces a rougher surface finish compared to the machined sample. The rougher pipe surface is more easily detectable as a surface feature by the stereovision camera when compared with the machined surface.

While the reconstruction of the surface (as shown on Fig. 18 using the data point (shown in Fig. 17)is capable to reconstruct the weld seam, finer details are lost due to the noise level of the data. To reduce the noise and obtain higher fidelity reconstruction, a better measurement workflow and refinement of the processing algorithm is required, which is beyond the scope of this study

When comparing the stitching procedure from data acquired from D405 RGB-depth camera and from laser triangulation, the notable characteristics is the type of data. As the data from the RGB-Depth camera is scattered along the center line of the pipe, it is possible to create surface map from a single frame from RGB-depth camera. However, the laser triangulation produce dataset which is a slice of the pipe contour in a single plane perpendicular to the pipe center line. With this limitation, it is impossible to create a surface map just from a single frame.

Ideally, the resulting surface data can then be used to identify particular defects individually. However, as it is now, it can only detect large sized features such as weld seam and weld cratering. Future improvement in the measurement system is targeted to enable detection of finer surface defect such as crack, spatters, or pitting.

The measurement is taken on weld sample from previous weld head test [10]. As the weld sample is used as it was produced by the welding head, the result is not controlled. Therefore a further testing with a controlled sample, possibly made using machining instead of welding, with controlled defect size and types, would be carried out as further development of this study and will be addressed in detail in future publications as more testing results are gathered.

4. Conclusion and outlook

From the measurement result, one of the main point is the effect odometry has on the measurement result. As shown in 3.1, slip has a detrimental effect on the stitching problem as this can change the distance between the measurement plane and therefore distort the detected feature on the pipe surface. Since the stereovision produce 3D data points along the surface for each measured frame, an algorithm can be developed further to match and error correct the error due to slip. This can then be compared with using odometry data. Result from the stereovision camera also requires further de-noising convolution to produce a surface map from the resulting point cloud.

On the other hand, as shown in 3.2, the laser only provides 2D annular data points on the pipe, therefore the data points cannot be used for self-correction. This makes the laser system more dependent on the reliability of the odometry system.

The next step of the PoP testing is to test the performance of the sensors with the odometry data taken. For Stereovision specifically, the additional step is to test the effect of the stitching correction using hardware (odometry data) and software (fitting correction).

In a previous study done at KIT, a critical surface defect size of $\pm 1\ mm^3$ is shown to be the maximum size limit for DEMO upper port pipes [8], therefore another step that needs to be done by the PoP test is to test the performance of the sensors in measuring the defect. A way to test this is to use synthetic sample with the surface defect machined in a controlled manner instead of using weld samples.

As was discussed in 3, at the current state both methods can only detect major features such as weld seam and major crater. Further development of this study is to take the planned odometry testing, and testing with synthetic sample and refine the measurement process to obtained higher fidelity images and surface maps. The goal of the higher fidelity images and surface maps is to be able to detect finer defects such as crack or pitting around the weld HAZ in sizes as small as $\pm 1\ mm^3$. furthermore, integration of this study in the overall DEMO maintenance concept is planned to develop a machine vision assisted algorithm (such as machine vision) to detect surface defects using the surface maps results.

Fig. 18. Reconstructed surface using data from Intel D405 camera (left) compared to the sample used (right).

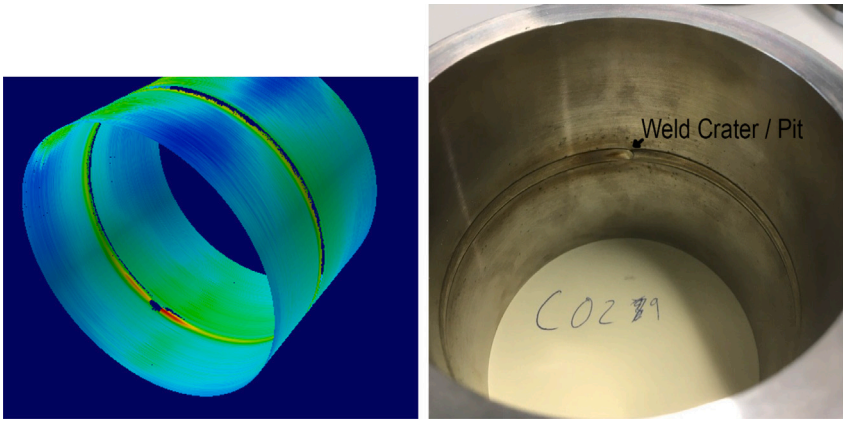

Fig. 19. Surface map of the pipe sample in 3D from laser triangulation method (left) compared with the sample used (right).

Funding sources

This research was funded by EUROfusion Consortium, funded by the European Union via the Euratom Research and Training Programme (Grant Agreement No 101052200 — EUROfusion).

Declaration of competing interest

The authors declare the following financial interests/personal relationships which may be considered as potential competing interests: Azman Azka reports financial support and administrative support were provided by European Consortium for the Development of Fusion Energy. Azman Azka reports a relationship with European Consortium for the Development of Fusion Energy that includes: funding grants. If there are other authors, they declare that they have no known competing financial interests or personal relationships that could have appeared to influence the work reported in this paper.

Acknowledgments

This work has been carried out within the framework of the EUROfusion Consortium, funded by the European Union via the Euratom Research and Training Programme (Grant Agreement No 101052200 — EUROfusion). Views and opinions expressed are however those of the author(s) only and do not necessarily reflect those of the European Union or the European Commission. Neither the European Union nor the European Commission can be held responsible for them.

Data availability

Data will be made available on request.

References

[1] O. Crofts, A. Loving, M. Torrance, S. Budden, B. Drumm, T. Tremethick, D. Chauvin, M. Siuko, W. Brace, V. Milushev, M. Mittwollen, T. Lehmann, F. Rauscher, G. Fischer, P. Pagani, Y. Wang, C. Baars, A. Vale, EU DEMO remote maintenance system development during the pre-concept design phase, Fusion Eng. Des. 179 (2022) 113121, http://dx.doi.org/10.1016/j.fusengdes.2022.113121, URL: https://www.sciencedirect.com/science/article/pii/S0920379622001211.

[2] M. Abdou, M. Riva, A. Ying, C. Day, A. Loarte, L.R. Baylor, P. Humrickhouse, T.F. Fuerst, S. Cho, Physics and technology considerations for the deuterium-tritium fuel cycle and conditions for tritium fuel self sufficiency, Nucl. Fusion 61 (1) (2021) 013001, http://dx.doi.org/10.1088/1741-4326/abbf35.

[3] T. Tremethick, S. Kirk, K. Keogh, A. O'Hare, E. Harford, B. Quirk, Service joining strategy for the EU DEMO, Fusion Eng. Des. 158 (2020) 111724, http://dx.doi.org/10.1016/j.fusengdes.2020.111724, URL: https://www.sciencedirect.com/science/article/pii/S0920379620302726.

[4] RSE-M: In-Service Inspection Rules for Mechanical Components of PWR Nuclear Islands, Association Francaise pour les regles de Conception, de construction et de surveillance en exploitation des materiels des Chaudieres Electro Nucleaires - AFCEN, 10, Rue Juliette Recamier, 69456 Lyon Cedex 06 (France), 2024, Editions AFCEN.

[5] R.W. Swayne, Section XI: Rules for inservice inspection and tests of nuclear power plant components, in: Online Companion Guide to the ASME Boiler and Pressure Vessel Codes, ASME Press, 2020.

[6] B.G. Bundesministerium der Justiz, KTA 3201.4 - Components of the primary loop of light water cooled reactors (LWR). Part 4. In- service inspection and monitoring. Version 6/99, Bundesanzeiger 51 (200a) (2025).

[7] C. Faidy, Nuclear in-service inspection codes ASME section XI and RSE-M codes comparisons, 2016, http://dx.doi.org/10.1115/PVP2016-63489, V01BT01A056.

[8] A. Azka, M. Mittwollen, Preliminary investigation of allowable weld defect size and orientation for DEMO cooling pipes, IEEE Trans. Plasma Sci. (2024) 1–4, http://dx.doi.org/10.1109/TPS.2024.3410009.
[9] R.A. Newcombe, S. Izadi, O. Hilliges, D. Molyneaux, D. Kim, A.J. Davison, P. Kohi, J. Shotton, S. Hodges, A. Fitzgibbon, Kinectfusion: Real-time dense surface mapping and tracking, in: 2011 10th IEEE International Symposium on Mixed and Augmented Reality, IEEE, 2011, pp. 127–136.
[10] K. Keogh, S. Kirk, W. Suder, I. Farquhar, T. Tremethick, A. Loving, Laser cutting and welding tools for use in-bore on EU-DEMO service pipes, Fusion Eng. Des. 136 (2018) 461–466, http://dx.doi.org/10.1016/j.fusengdes.2018.02.098, Special Issue: Proceedings of the 13th International Symposium on Fusion Nuclear Technology (ISFNT-13). URL: https://www.sciencedirect.com/science/article/pii/S0920379618302084.
[11] NI Vision Concepts Manual, National Instruments Corporation, Austin, TX, 2024, https://www.ni.com/docs/de-DE/bundle/ni-vision-concepts-help/page/nivisionconcepts.html.
[12] D. Nair, A guide to stereovision and 3D imaging, NASA Tech Briefs 36 (10) (2012).
[13] A. Donges, R. Noll, Laser measurement technology: Fundamentals and applications, in: Springer Series in Optical Sciences, Springer Berlin Heidelberg, 2014.
[14] H. Rostam Affendi, I. Haidi, Literature survey on stereo vision disparity map algorithms, J. Sensors 2016 (2016) 1–23, http://dx.doi.org/10.1155/2016/8742920, URL: https://cir.nii.ac.jp/crid/1363951794953852928.
[15] F.K. Noble, Comparison of opencv's feature detectors and feature matchers, in: 2016 23rd International Conference on Mechatronics and Machine Vision in Practice, M2VIP, 2016, pp. 1–6, http://dx.doi.org/10.1109/M2VIP.2016.7827292.
[16] Intel, Intel® RealSense™ product family D400 series, 2024, Brochure.
[17] M. Munaro, E. So, S. Tonello, E. Menegatti, Efficient completeness inspection using real-time 3D color reconstruction with a dual-laser triangulation system, Adv. Comput. Vis. Pattern Recognit. 48 (2015) 201–225, http://dx.doi.org/10.1007/978-1-4471-6741-9_7.
[18] M. Jacob, M. Unser, Design of steerable filters for feature detection using canny-like criteria, IEEE Trans. Pattern Anal. Mach. Intell. 26 (8) (2004) 1007–1019, http://dx.doi.org/10.1109/TPAMI.2004.44.